



ISSN 1110-0451



(E S N S A)

Analysis of Alpha Elastically Scattered by Light Nuclei Using Crystalline Model Approach

A. Amar^{1*} and Maha Selim²

⁽¹⁾ Physics Department, Faculty of Science, Tanta University, Tanta, Egypt

⁽²⁾ Mathematics Department, Faculty of Science, Tanta University, Tanta, Egypt

ARTICLE INFO

Article history:

Received: 25th July 2021

Accepted: 14th Dec. 2021

Keywords:

Crystal Model,

Coupled Reaction Channel,

Volume integral.

ABSTRACT

Elastic scattering of alpha particles by light nuclei is achieved using coupled reaction channel (CRC) and crystalline model approach (CM) to compare and reanalyze the availability of applying novel ideas in the nuclear reaction field. Coupled reaction channel (CRC) and crystal model (CM) have been used on alpha elastically scattered by ${}^6\text{Li}$, ${}^9\text{Be}$, and ${}^{11}\text{B}$, where alpha–target interaction has been modified. The real part of the potential has been selected as crystal model (CM) with a Gaussian form. The imaginary part of the potential was taken in Woods-Saxon form, where the spin-orbit effect has been excluded from this analysis. Fitting of experimental data obtained using CRC and CM agreed well for alpha elastically scattered by ${}^6\text{Li}$ and ${}^9\text{Be}$, whereas results obtained for ${}^{11}\text{B}$ using CM were poor. More modifications should be made on CM to reproduce the differential cross-section for alpha elastically scattered by ${}^{11}\text{B}$.

1. INTRODUCTION

The light nuclei as ${}^6\text{Li}$, ${}^7\text{Be}$, and ${}^{10,11}\text{B}$ tend to form nuclei clusters, which provide an opportunity to study them in cluster folding, coupled reaction channel (CRC), and crystal model (CM) [1–3]. CM [3] provides a relation for the cluster interaction (using an arbitrary constant) with the distance for light nuclei ${}^6\text{Li}$ and ${}^7\text{Be}$. It indicates the need to modify the model to be suitable for a more complicated process for studying the elastic scattering of light particles by ${}^6\text{Li}$, ${}^9\text{Be}$, and ${}^{11}\text{B}$. Nuclear physicists and astrophysicists aim to discover the mechanism of nuclear reactions and the structure of the nucleus [4]. Starting from the liquid drop model, many models have been proposed to discover the structure and mechanisms of nuclear reactions, where each model has its availability to interpret a range of atomic numbers and others for the range of forward and backward angles. Several attempts have been made on nuclear systems to overcome ambiguities in nuclear parameters (optical parameters [OMPs], spectroscopic factor [SF], asymptotic normalization coefficient [ANC], and astrophysical S-factor); for example, coupled-cluster approach [5–8] and coupled channel scattering [9–12] are studied using lattice calculations at the crystal lattice range in the Fermi scale.

Rupak and Lee performed nuclear reaction calculations on the crystal lattice using the general method, and a radiative reaction (n,γ) on the lattice has been achieved. Here, they included ${}^{14}\text{C}(n,\gamma){}^{15}\text{C}$ as an example of the applicability of their theory by calculating photonuclear reaction rates in the lattice [13]. Meißner has investigated clustering by applying the ab initio method on the lattice where alpha clustering was the core of the research because of the properties of alpha particles as high binding energy and spin (isospin) saturated for ${}^{12}\text{C}$ [14]. The nuclear lattice simulation method has been used to explain the clustering in lattice without constraints, presenting this method as a benchmark for ab initio calculations using chiral nuclear effective field theory (EFT) [4]. Matter nuclear distribution for ${}^6\text{Li}$, ${}^6\text{He}$, and ${}^9\text{Be}$ has been rearranged as nuclear density distribution [3] to be suitable for studying light nuclei. The binding energy and nuclear density distribution have been calculated for light nuclei depending on alpha as a core of the cluster. They selected ${}^6\text{Li}$ and ${}^6\text{He}$ as $(\alpha + n + n)$ and ${}^9\text{Be}$ as $\alpha + \alpha + n$; however, for ${}^6\text{Li}$, it was an approximation to select neutrons instead of protons in the configuration [3]. Jenson et al. have summarized the form of the nuclear density distribution of light nuclei in the form of the summation of two Gaussians [15].

Optical model can reproduce the differential cross-section at forward angles with phenomenological treatment for many nuclear systems. Studying light nuclei elastically scattered by light nuclei gives an opportunity to apply different models to investigate the structure of the interacting nuclei. Alpha, elastically scattered by ${}^6\text{Li}$, ${}^9\text{Be}$, and ${}^{11}\text{B}$, has been widely used to examine the structure of the nuclei under consideration. It has been suggested that [2] light nuclei tend to form clusters, where there are many probabilities for such forms. CRC is the ideal method to survey the entire range of angles, where involving the transfer with elastic scattering is used to extract spectroscopic amplitude for the configuration. The binding energy can also be adjusted from the fitting process of experimental data by changing it to reproduce the differential cross-section.

A new approach [3] has been attempted to investigate the nuclear systems, where the real part has the form in equation (1) in the second section. The modified potential has been selected from the projectile parameters (atomic and mass number) where the potential of the target has been neglected. Here, the attractive force between all nucleons has been represented in the second term of equation (1). The importance of such a study appears when one form of potential succeeded in reproducing the differential cross-section for alpha elastically scattered by ${}^6\text{Li}$, ${}^9\text{Be}$, and ${}^{11}\text{B}$.

Almost all the nuclei studied in the present article are weakly bound. This study modifies the interaction potential from CM for alpha elastically scattered by light nuclei. The suggested potential is used as the real part of optical potential, and the imaginary part is adopted from the literature.

2. MODELING

A new potential form has been suggested using CM to investigate alpha particles with light nuclei ${}^6\text{Li}$, ${}^9\text{Be}$, and ${}^{11}\text{B}$ with the form:

$$V_{CM}(R) = -V_0 \text{Exp}[a(\frac{R}{r_0})^2 - b(\frac{R}{r_0})^2] \quad (1)$$

where $a = 2$, $b = 4$, and $r_0 = 1.5\text{fm}$ for alpha particles. Here, a represents the number of protons, b represents the atomic number of alpha particles, and r_0 is the nucleon radius. Eq. (1) describes the real part of the alpha-target interaction. It can be obtained from the nonrelativistic Schrödinger equation:

$$H\psi = \left(-\frac{\hbar}{2\mu} \nabla^2 + U(R) \right) \psi(R) = E\psi(R) \quad (2)$$

where μ is the reduced mass of the projectile and target and E is the energy of the relative motion in the center of the mass system. The analytical expression used for the phenomenological optical model in this study has the form:

$$U(R) = V_{CM}(R) + iW(R) + V_C(R) \quad (3)$$

where $V_{CM}(R)$ is the real part of the potential, $W(R)$ is the imaginary part of the potential, and $V_C(R)$ is the Coulomb part of the potential. The Woods–Saxon (WS) form has been selected for the imaginary part. The real part has a semi-microscopic potential with the general form given as follows:

$$Wf(R_v, r, a_v) = -W_0(1 + \exp(\frac{r-R_v}{a_v}))^{-1} \quad (4)$$

where the form factor is the WS form:

$$f(R_i, r, a_i) = (1 + \exp(\frac{r-r_i A_i^{\frac{1}{3}}}{a_i}))^{-1}, i = W \quad (5)$$

3. RESULTS AND DISCUSSION

3.1 Alpha elastically scattered by ${}^6\text{Li}$

The CM approach is used to obtain the density distribution of ${}^6\text{Li}$, ${}^7\text{Li}$, and ${}^7\text{Be}$ nuclei selected as a Gaussian distribution. The first term is an alpha cluster, and the second Gaussian represents the residual cluster of the nucleus. For example, ${}^6\text{Li}$ is taken as $d + \alpha$ or $t + {}^3\text{He}$ (two configurations with the same probabilities). The density distribution of ${}^6\text{Li}$ now is a summation of two Gaussian distributions, one for deuteron and the other for alpha. This can be described for ${}^7\text{Li} = \alpha + t$ configuration as in the cluster structure. Thus, the alpha will be the core of the nucleus and triton as valence (Fig. 1a, and 1b).

The potential $V(r)$ has been included in the Fresco program [16] as a real part, whereas the imaginary part has been selected from the literature. This potential represents the interaction between alpha and any light targets.

CRC calculation where taken for elastic scattering and elastic scattering with transfer. For example, in case of alpha elastically scattered by ${}^6\text{Li}$ with deuteron transfer has been included at backward angles to interpret the anomalous large angle scattering (ALAS) phenomenon. The break-up has been noticed with a significant effect as ${}^6\text{Li}$ is weakly bound nuclei and the effect will be studied in another work at near future.

The form of the bound state potential has a significant effect on the fitting of experimental data.

The bound state potential [17] CM is used as the real part, whereas the imaginary part is selected from the phenomenological analysis obtained from the energy experimental data under consideration using the Fresco program. Spectroscopic amplitude of ${}^6\text{Li}(\alpha, {}^6\text{Li})\alpha$ has been extracted from the experimental data at $E_\alpha = 18, 29.4, 36.6, 45, 50.9, 59, 104, \text{ and } 166 \text{ MeV}$. The extracted spectroscopic amplitudes of ${}^6\text{Li} \equiv \alpha + d$ configuration using CM and CRC are shown in Table 1. The extracted spectroscopic amplitudes from CM differ from those extracted from CRC indicating the effect of different models on the spectroscopic information. CRC can enhance the fitting of experimental data, especially at backward angles (Fig 3). The suggested model (CM) succeeded in reproducing the differential cross-section for experimental data at $E_\alpha = 18, 29.4, 36.6, 45, 50.9, 59, 104, \text{ and } 166 \text{ MeV}$. The analysis has adjusted the fitting using CM, especially at 29 MeV; however, CRC could not reproduce the differential cross-section at the specified experimental data (Fig. 3). Analysis showed that CRC could reproduce the differential cross-section for alpha elastically scattered by ${}^6\text{Li}$, where experimental data were taken from previous publications [18–29].

The obtained parameters for crystal model and coupled reaction channel are shown in Table (1). The energy dependences of real volume integral and for imaginary volume integral are shown in Fig. (7) and could be expressed respectively as $J_v = 276.267 - 0.168 E_\alpha$, and $= -19.45 + 3.7374E$. As the Q-value of ${}^6\text{Li} \equiv \alpha + d$ ($Q = -28.30 \text{ MeV}$) is large so, the deuteron cluster exchange model is expected to be more important at higher incident energy. The deuteron transfer with elastic scattering of ${}^6\text{Li}(\alpha, \alpha){}^6\text{Li}$ at higher energies 166MeV could be used to extract a reliable spectroscopic

amplitude of ${}^6\text{Li} \equiv \alpha + d$. The extracted spectroscopic amplitude of ${}^6\text{Li} \equiv \alpha + d$ is shown in Table (1). The extracted spectroscopic amplitude value (0.50) of ${}^6\text{Li} \equiv \alpha + d$ is quite small in comparison with calculated value (1.061). The choice of energy for study was for energies where deuteron transfer is very obvious at backward angles and effective during the analysis.

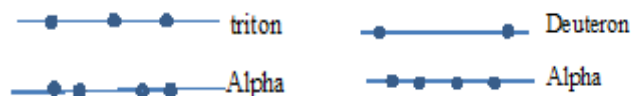


Fig. (1a): Cluster model distribution for ${}^7\text{Li}$ and ${}^6\text{Li}$

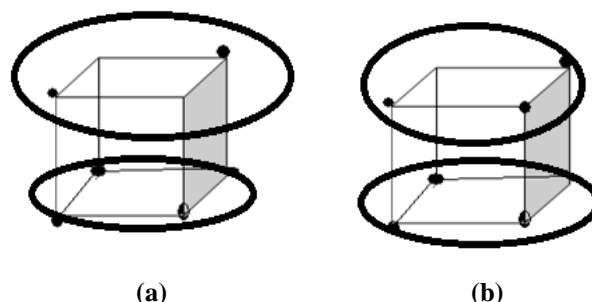


Fig. (1b): Crystal model distribution of nucleons for ${}^6\text{Li}$ where a) ${}^6\text{Li}$ is taken as alpha on the base and deuteron on the upper face, and b) ${}^7\text{Li}$ is taken as alpha on the base and triton on the upper face (hypothetical case as Actually, 6 or ${}^7\text{Li}$ interaction points do not have a cubic form. A simple cubic lattice is an unstable configuration for these two cases where the rings represent the hypothetical shape of the clusters distribution on the lattice)

The first channel in CRC reaction channel was inelastic scattering of $d + {}^6\text{Li}^*$ with elastic scattering. The second, was alpha transfer with elastic scattering.

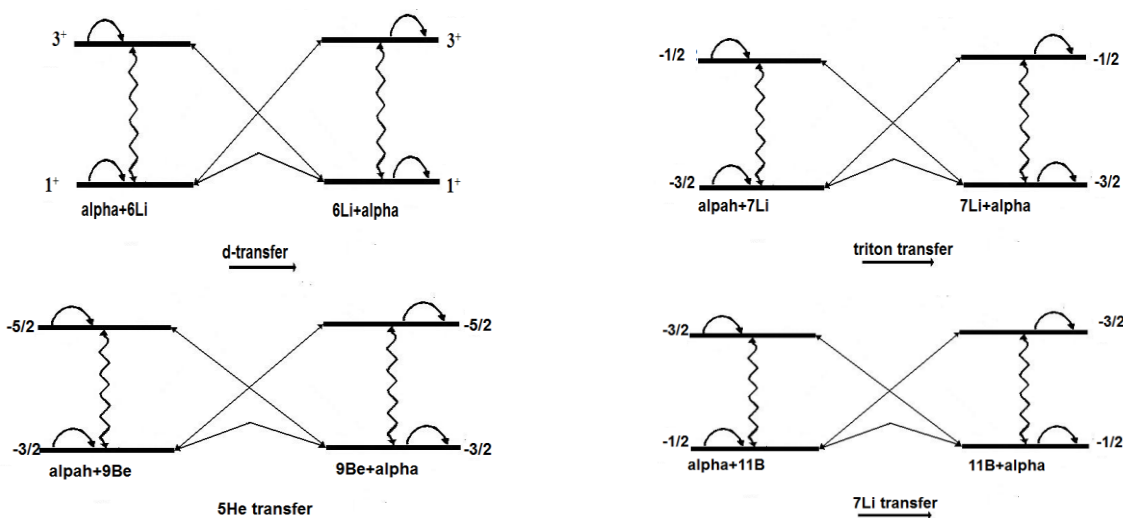


Fig. (2): The coupling scheme used in calculations of ${}^4\text{He}$ elastic scattering on ${}^6\text{Li}$ nuclei using coupled reaction channels method

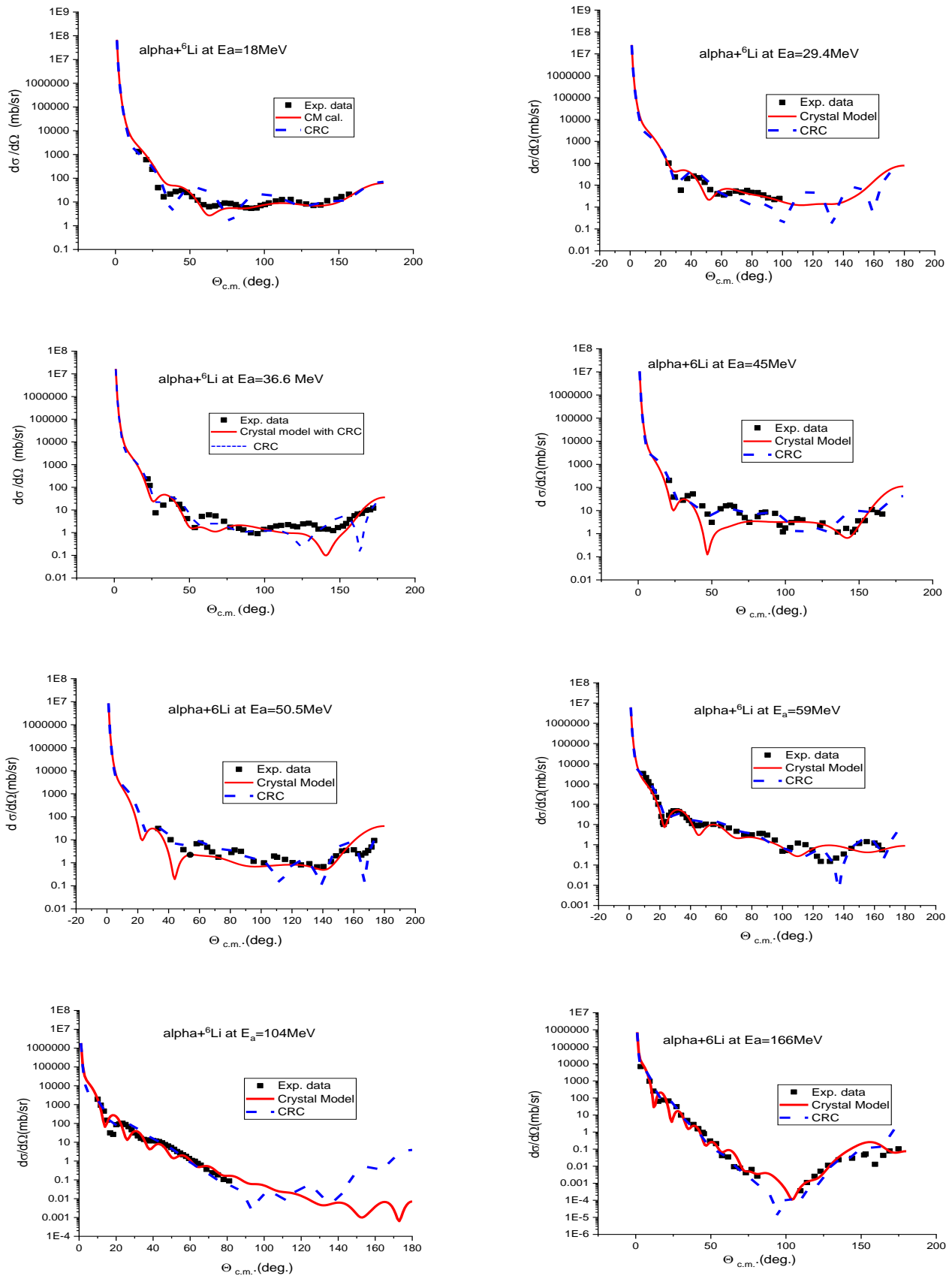


Fig. (3): Angular distribution for alpha elastically scattered by ${}^6\text{Li}$; square dots represent experimental data, dashed line represents CRC calculations, and the line represents the calculated results using CM

Table (1): Parameters obtained for alpha elastically scattered by ${}^6\text{Li}$ with a fixed r_c at 1.3 fm for CM calculations

E_α MeV		V_0 , MeV	r_0 , fm	a_0 , fm	W_v , MeV	r_v , fm	a_v , fm	J_v MeV.fm ³	J_w MeV.fm ³	SA	σ_R , mb
18.00	CRC	113.00	1.15	0.78	10.00	1.17	0.65	343.6	24.86	0.80	453.6
	CM	Nr=0.40			05.77	1.170	0.650			2.00	
36.60	CRC	120.00	1.15	0.78	21.74	1.11	0.65	364.8	48.96	0.56	798.3
	CM	Nr=0.52			08.77	1.170	0.650			0.85	
29.00	CRC	126.00	1.15	0.78	21.00	1.11	0.65	383.0	75.58	0.56	826.1
	CM	Nr=0.40			14.77	1.110	0.650			2.0	
45.00	CRC	115.00	1.15	0.78	11.74	1.17	0.65	349.7	63.54	0.56	686.2
	CM	Nr=0.20			05.77	1.170	0.650			0.90	
50.50	CRC	115.00	1.15	0.78	11.74	1.17	0.65	334.6	29.84	0.56	723.6
	CM	Nr=0.50			05.77	1.170	0.650			0.70	
59.00	CRC	110.00	1.15	0.78	17.00	1.17	0.65	332.5	91.77	0.56	670.2
	CM	Nr=0.40			13.50	1.170	0.25			0.25	
104.00	CRC	90.00	1.15	0.78	16.00	1.17	0.65	272.0	39.78	0.45	579.6
	CM	Nr=0.40			70.50	1.170	0.50			1.00	
166.00	CRC	85.00	1.15	0.78	21.00	1.17	0.65	256.9	113.3	0.50	567.1
	CM	Nr=0.40			21.50	1.170	0.50			0.50	

3.2 Alpha elastically scattered by ${}^7\text{Li}$

The crystal model approach (CM) has been applied on alpha elastically scattered by ${}^7\text{Li}$ for the available experimental data. The model succeeded in reproducing the differential cross-section at the entire range of study. The ${}^7\text{Li}$ nucleus was taken to be alpha+ triton clusters, which is used in this study as one configuration among many of them (${}^7\text{Li} \equiv {}^1\text{H} + {}^6\text{He}$, ${}^2\text{H} + {}^5\text{He}$, ${}^3\text{H} + {}^4\text{He}$, and ${}^1\text{n} + {}^6\text{Li}$). These configurations have different probabilities in CM, which should be examined depending on the experimental data. The potentials for alpha elastically scattered by alpha and deuteron were taken from the global optical potential for alpha projectile [30]. The choice of the bound state potential is essential. The ${}^7\text{Li} \equiv {}^3\text{H} + {}^4\text{He}$ configuration has been examined in this analysis, whereas the remaining configurations need further investigation.

The comparison between the experimental data for $\alpha+{}^7\text{Li}$ nuclear system at energies 12- 65 MeV and the theoretical calculations within the framework of CM and CRC using FRESKO code is shown in Fig. 4. The CM analysis was carried out by optimizing two free parameters, for imaginary WS potential (W_v , a_v) where the radii $r_o = 1.281$ fm and $r_v = 1.34$ fm were fixed.

In CRC analysis, the parameters of the imaginary WS potential that resulted from CM analysis were kept fixed and allowing only one parameter – the real renormalization factor N_r – to be changed freely. The radius parameter for the Coulomb potential (r_c) was fixed at 1.3 fm. The CM and CRC potential parameters, the values of real (J_v) and imaginary (J_w) volume integral as well as reaction cross sections are listed in Table 2. Both CM and CRC calculations give equally good fitting to the data compared to the data fitting in its original published paper. The depth of the imaginary part has been modified to reproduce the differential cross-section. The bound state potential shape has a significant effect on the differential cross-section reproduction at the backward angles. Moreover, the transfer of triton with elastic scattering was investigated using distorted wave born approximation (DWBA) + CM calculation, where the parameters of the fitting process are presented in Table (2). The real part is taken as CM, whereas the imaginary part was included in the analysis from global optical parameters of alpha as a projectile from the literature [30]. Fig. (4) shows the comparison of theoretical analysis and experimental data for alpha elastically scattered by ${}^7\text{Li}$.

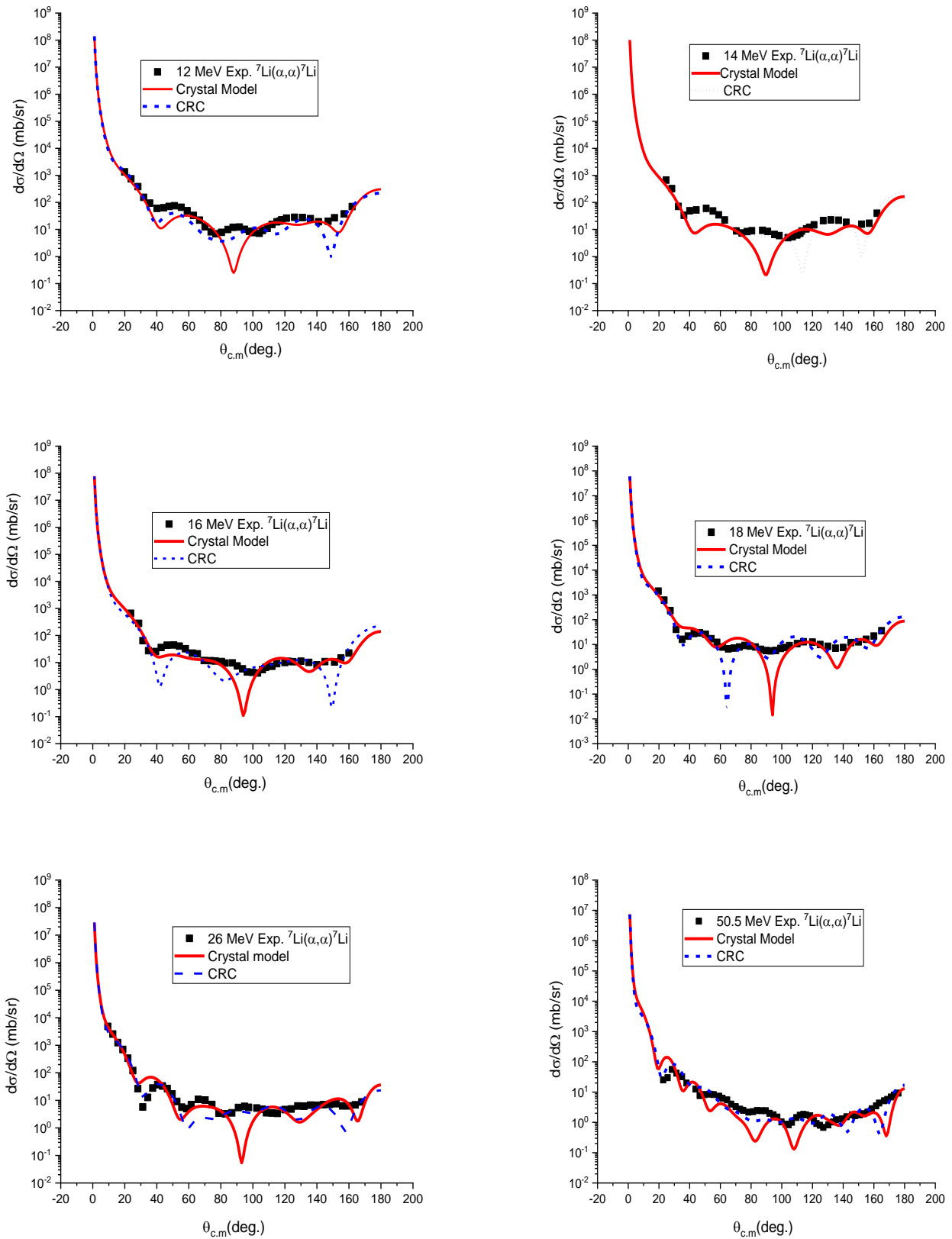


Fig. (4): Angular distribution for alpha elastically scattered by ${}^7\text{Li}$; square dots represent experimental data, dashed line represents CRC calculations, and line represents the calculated results using CM, where experimental data were taken from previous publications [19,31,32]

Table (2): Parameters obtained for alpha elastically scattering by ${}^7\text{Li}$ with a fixed r_c at 1.3 fm for CM calculations

E_α MeV		V_0 , MeV	r_0 , fm	a_0 , fm	W_v , MeV	r_v , fm	a_v , fm	J_v MeV.fm ³	J_w MeV.fm ³	SA	σ_R , mb
12.00	CRC	124.8	1.28	0.79	07.56	1.34	0.5	559.99	26.6	0.90	1127.
	CM	Nr=0.3			07.56	1.34	0.65			1.40	923.8
14.00	CRC	137.8	1.28	0.68	06.32	1.34	0.5	535.58	28.9	0.60	756.3
	CM	Nr=0.30			06.32	1.34	0.65			1.30	921.2
16.00	CRC	175.9	1.28	0.50	13.57	1.34	0.5	547.10	47.1	0.90	1503.
	CM	Nr=0.30			13.57	1.34	0.50			1.40	921.4
18.00	CRC	132.94	1.28	0.80	17.62	1.34	0.5	605.43	61.1	0.90	895.2
	CM	Nr=0.25			25.62	1.34	0.50			1.50	1035.
26.00	CRC	158.9	1.28	0.64	20.62	1.34	0.5	590.6	45.24	0.20	811.0
	CM	Nr=0.40			22.62	1.34	0.50			1.80	1039.
50.00	CRC	141.9	1.28	0.72	36.62	1.34	0.698	587.23	160.5	0.70	847.7
	CM	Nr=0.90			47.62	1.34	0.50			1.60	1176.

3.3 Alpha elastically scattered by ${}^9\text{Be}$

${}^9\text{Be}$ has a significant position between *Ip-shell* nuclei, where the structure is known as Borromean structure. Light nuclei such as ${}^6\text{Li}$, ${}^9\text{Be}$, and ${}^{10,11}\text{B}$ tend to form clusters, and ${}^9\text{Be}$ has the configurations $\alpha + {}^5\text{He}$, $d + {}^7\text{Li}$, $t + {}^6\text{Li}$, and $n + {}^8\text{Be}$. Each configuration has its probability. The analysis of alpha elastically by ${}^9\text{Be}$ scattered has been conducted in the CM framework with ${}^5\text{He}$ transfer. The extracted spectroscopic amplitudes obtained from the experimental data using CM are presented in Table 3. The elastic scattering for ${}^9\text{Be}(\alpha, \alpha){}^9\text{Be}$ was conducted in the CRC framework. Here, ${}^5\text{He}$ transfer ${}^9\text{Be}(\alpha, {}^9\text{Be})\alpha$ at backward angles was investigated for the entire range of angles. The modifications of the real and imaginary parts of the potential have been conducted to reproduce the differential cross-section for ${}^9\text{Be}(\alpha, \alpha){}^9\text{Be}$ and ${}^9\text{Be}(\alpha, {}^9\text{Be})\alpha$. CM+DWBA can reproduce the differential cross section at the entire range of angles, even at backward angles ${}^9\text{Be}(\alpha, {}^9\text{Be})\alpha$ (Fig. 5).

It is believed that light nuclei tend to be into clusters as ${}^9\text{Be}=(\alpha+{}^5\text{He}, d+{}^7\text{Li}, t+{}^6\text{Li}, \text{ and } n+{}^8\text{Be})$. The configuration $n+{}^8\text{Be}$ has been thought to have the higher

probability than other configurations [35], $n+{}^8\text{Be}$ configuration has a probability 68.7% where $\alpha+{}^5\text{He}$ configuration has only 25.1% from total probability of ${}^9\text{Be}$ cluster configurations. Borromean structure of ${}^9\text{Be}$ has been investigated in many studies. ${}^9\text{Be}$ is thought to be a weakly bound nucleus resulting from Borromean structure which is expected to break up into $n+ \alpha, n+{}^8\text{Be}$ (2α in 10^{-16}sec) or may through ${}^5\text{He}$ or ${}^8\text{Be}$ (which unstable nuclei). The effect of ${}^5\text{He}$ transfer with elastic scattering has been included into coupled reaction channel calculation on ${}^9\text{Be}(\alpha, \alpha){}^9\text{Be}$ and ${}^9\text{Be}(\alpha, {}^9\text{Be})\alpha$ for whole range of angles. Also, the effect of including inelastic scattering on optical parameters and spectroscopic amplitude has been done for ${}^9\text{Be}=\alpha+{}^5\text{He}$ configuration. The depth of real and imaginary potential part have been justified to reproduce differential cross section for ${}^9\text{Be}(\alpha, \alpha){}^9\text{Be}$ and ${}^9\text{Be}(\alpha, {}^9\text{Be})\alpha$ at energies under consideration. The optical model is able to reproduce forward angles differential cross section where backward angles need sophisticated models. At backward angles ${}^9\text{Be}(\alpha, {}^9\text{Be})\alpha$, coupled reaction channel has been applied as shown in Fig.(5)

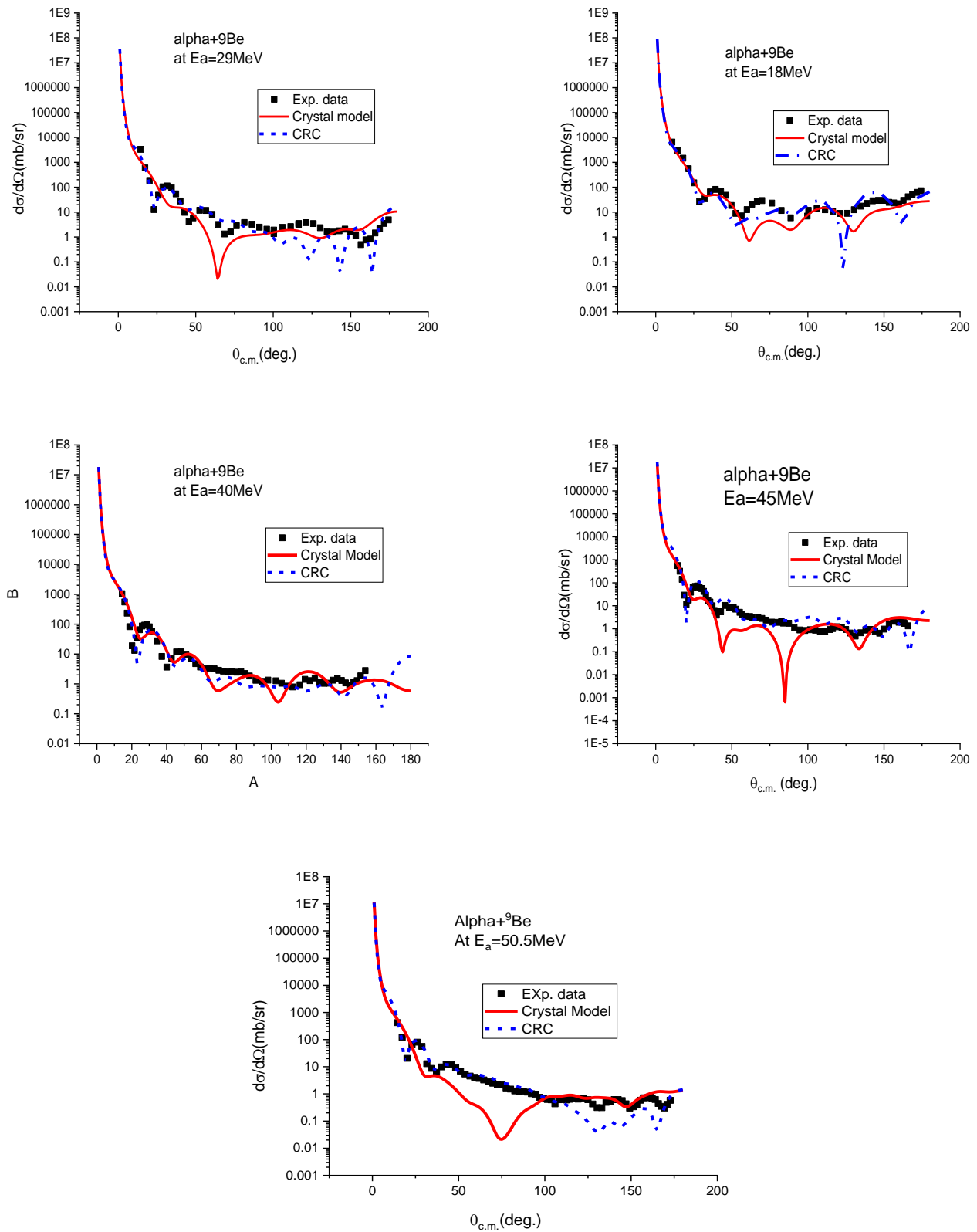


Fig. (5): Angular distribution for alpha elastically scattered by ${}^9\text{Be}$, square dots represent the experimental data, dashed line represents the CRC calculations, and line represents the calculated results using CM, where experimental data were taken from other publications [33–38]

Table (3): Parameters obtained for alpha elastically scattering by ${}^9\text{Be}$ with a fixed r_c at 1.3 fm for CM calculations

E_α MeV		V_0 , MeV	r_0 , fm	a_0 , fm	W_v , MeV	r_v , fm	a_v , fm	J_v MeV.fm ³	J_w MeV.fm ³	SA	σ_R , mb
18.00	CRC	98.8	1.45	0.80	08.82	1.30	0.757	397.8	26.93	1.00	961.87
	CM	Nr=0.65			09.06	1.345	0.65			1.80	1013.5
29.00	CRC	095.0	1.45	0.80	40.44	1.306	0.70	386.8	115.8	0.75	1073.6
	CM	Nr=0.40			13.06	1.345	0.30			2.00	822.17
40.00	CRC	81.0	1.38	0.73	40.06	1.051	0.990	277.0	132.9	1.25	1075.7
	CM	Nr=0.90			10.06	1.345	0.25			1.56	768.32
45.00	CRC	79.0	1.45	0.73	29.44	1.306	0.90	286.0	114.0	1.00	1044.2
	CM	Nr=0.90			05.06	1.345	0.40			2.00	703.72
50.00	CRC	79.0	1.45	0.73	29.44	1.306	0.90	289.9	116.9	1.20	1019.4
	CM	Nr=0.50			18.06	1.345	0.65			1.40	518.56

3.4 Alpha elastically scattered by ${}^{11}\text{B}$

The analysis of the experimental data for alpha elastically scattered by ${}^{11}\text{B}$ at 29–54 MeV [39–42] has been achieved in CRC and CM frameworks. CRC analysis of the experimental data was performed using WS forms for the real and imaginary parts of the potential. Here, the radii $r_o = 1.281 \text{ fm}$ and $r_v = 1.34 \text{ fm}$ were fixed and only the parameters (V_o , W_v , a_o , a_v) were taken as variables. The potential parameters were optimized by reproducing the experimental differential cross-section in all calculations. The N_r “renormalization factor for the real part” has been changed in addition to the imaginary part of the potential to obtain the best fit for the experimental data. The coulomb potential radius (r_c) was fixed at 1.3 fm during calculations. The optimal potential parameters extracted from CRC and CM calculations, the values of the real (J_v) and imaginary (J_w) volume integrals, and the values of reaction cross-sections σ_R for the energies under consideration are presented in Table (4). Fig. (6) shows the comparison between the experimental data and the theoretical calculations at the energies under considerations using CRC and CM. The real volume integral (J_v) decreases with increasing energy, whereas the imaginary volume integral (J_w) increases with increasing energy (Table 4). The energy dependences of the real volume and imaginary volume integrals are presented in Fig7. The experimental data were taken from [39–42].

In other words, the fitting process was performed using only one free parameter N_r “renormalization factor

for the real part”. The optimal potential parameters extracted from both OM and DFM calculations, the values of real (J_v) and imaginary (J_w) volume integrals as well as the values of reaction cross sections σ_R for the six studied energies are listed in Table 4. The comparison between the experimental data and the theoretical calculations at the different concerned energies utilizing both CM and CRC are presented in Fig. 6. Both CM and CRC calculations reasonably reproduce the data in the whole angular range. The energy dependences of real volume integral and for imaginary volume integral are shown in Fig.7. As shown in Table 4, the extracted N_r values for $\alpha+{}^{11}\text{B}$ system ranges between 0.20 and 0.60 with average value 0.40. The obtained real volume integrals extracted from CM and CRC calculations are very close with an average difference by $\pm 0.2\%$. The experimental angular distributions in the energy range from 40 to 65 MeV presents an airy minimum pattern, which considered a characteristic feature of elastic $\alpha+{}^{11}\text{B}$ nuclear system as shown in Fig. 6. The positions of airy minimum pattern shifted to smaller angles in the forward angular region by increasing the energy of alpha particles. CM analysis has been done without any transfer for $\alpha+{}^{11}\text{B}$ nuclear system. Coupled reaction channel for $\alpha+{}^{11}\text{B}$ has been used at all energies under considerations which could reproduce differential cross section. Alpha elastic scattering by ${}^{11}\text{B}$ with ${}^7\text{Li}$ transfer has been used in the present analysis to analyze backward angles.

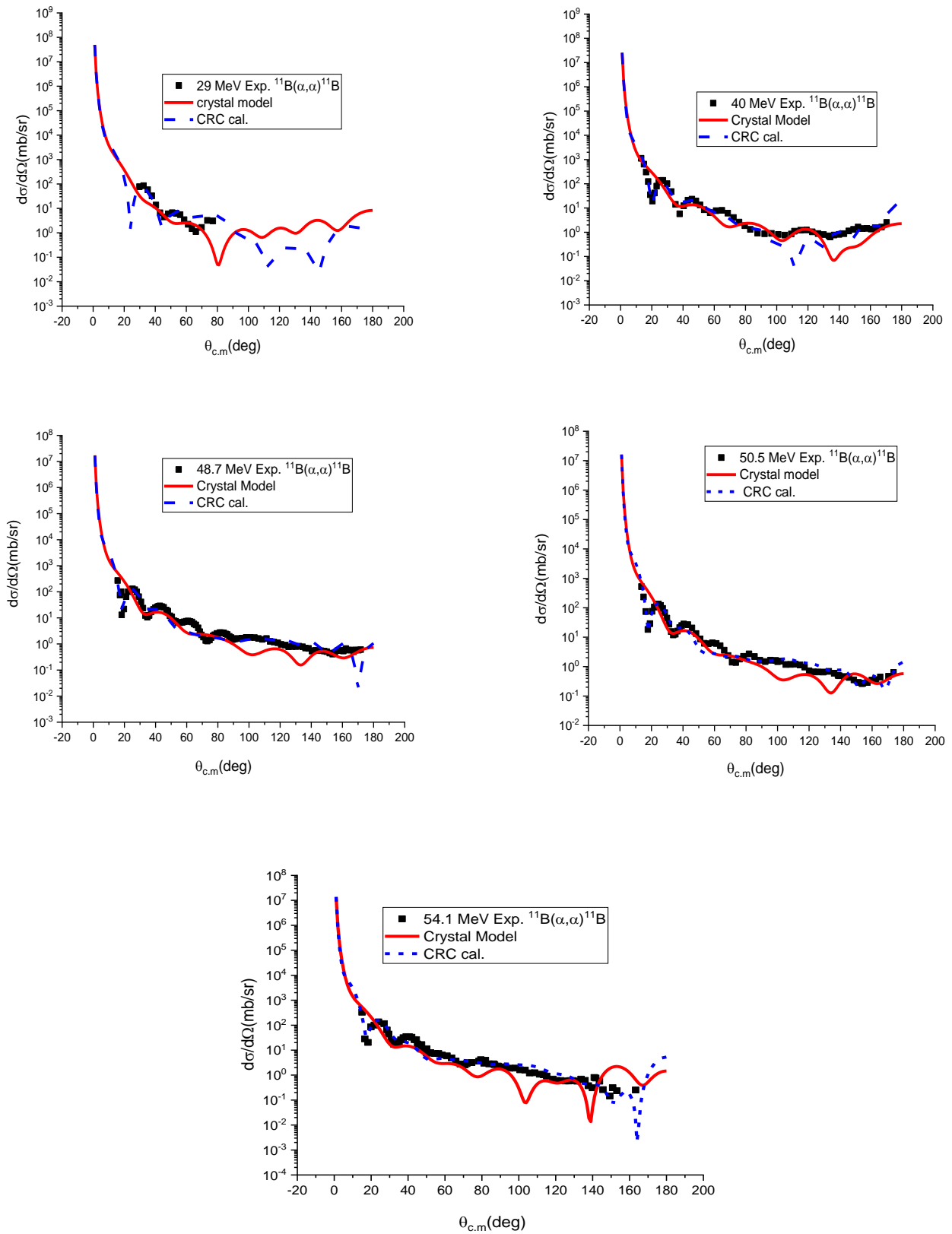
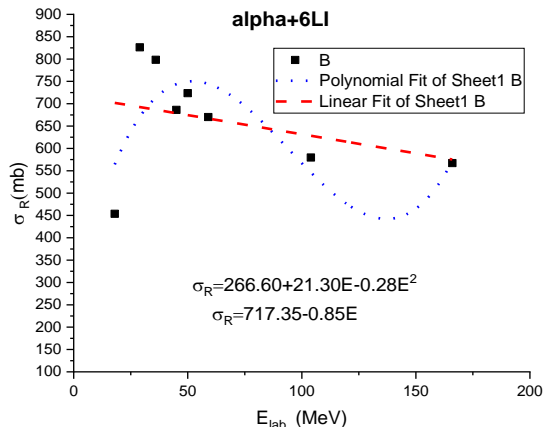
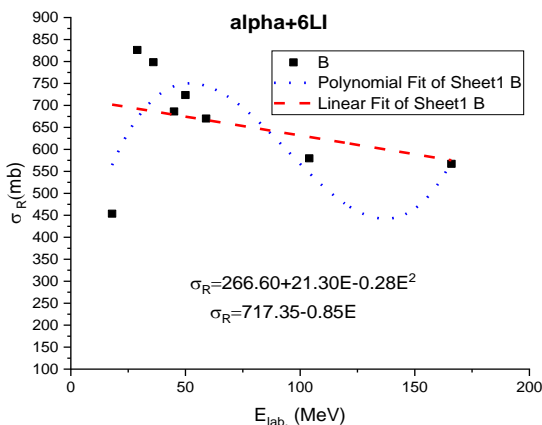
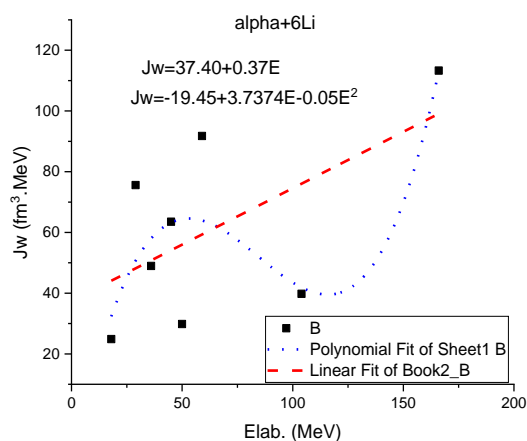
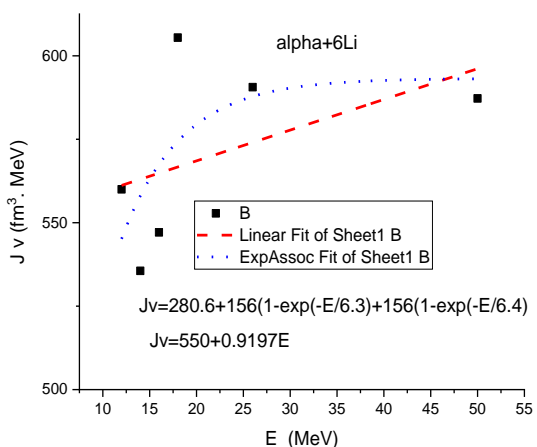


Fig. (6): Angular distributions for alpha elastically scattered by ^{11}B , square dots represent the experimental data, dashed line represents CRC calculations, and line represents the calculated results using CM

Table (4): Parameters obtained for alpha elastically scattering by ¹¹B with a fixed r_c at 1.3 fm for calculations where CM is crystal model calculations

E _α MeV		V ₀ , MeV	r ₀ , fm	a ₀ , fm	W _v , MeV	r _v , fm	a _v , fm	J _v MeV.fm ³	J _w MeV.fm ³	SA	σ _R , mb
29.00	CRC	130.4	1.28	0.69	23.35	1.34	0.722	442.55	44.76	0.80	970.7
	CM	Nr=0.60			23.35	1.340	0.722			1.20	
40.00	CRC	126.4	1.28	0.73	27.35	1.34	0.675	439.60	53.86	0.69	936.2
	CM	Nr=0.40			25.35	1.340	0.20			0.65	
48.70	CRC	115.2	1.28	0.72	28.35	1.34	0.691	406.61	109.1	0.65	891.0
	CM	Nr=0.20			30.35	1.340	0.20			0.65	
50.50	CRC	114.4	1.28	0.73	27.35	1.34	0.755	408.88	112.2	0.69	937.0
	CM	Nr=0.20			30.35	1.340	0.20			0.65	
54.10	CRC	114.2	1.28	0.72	24.85	1.34	0.698	414.57	103.2	0.65	856.7
	CM	Nr=0.20			27.35	1.340	0.20			1.10	



continue

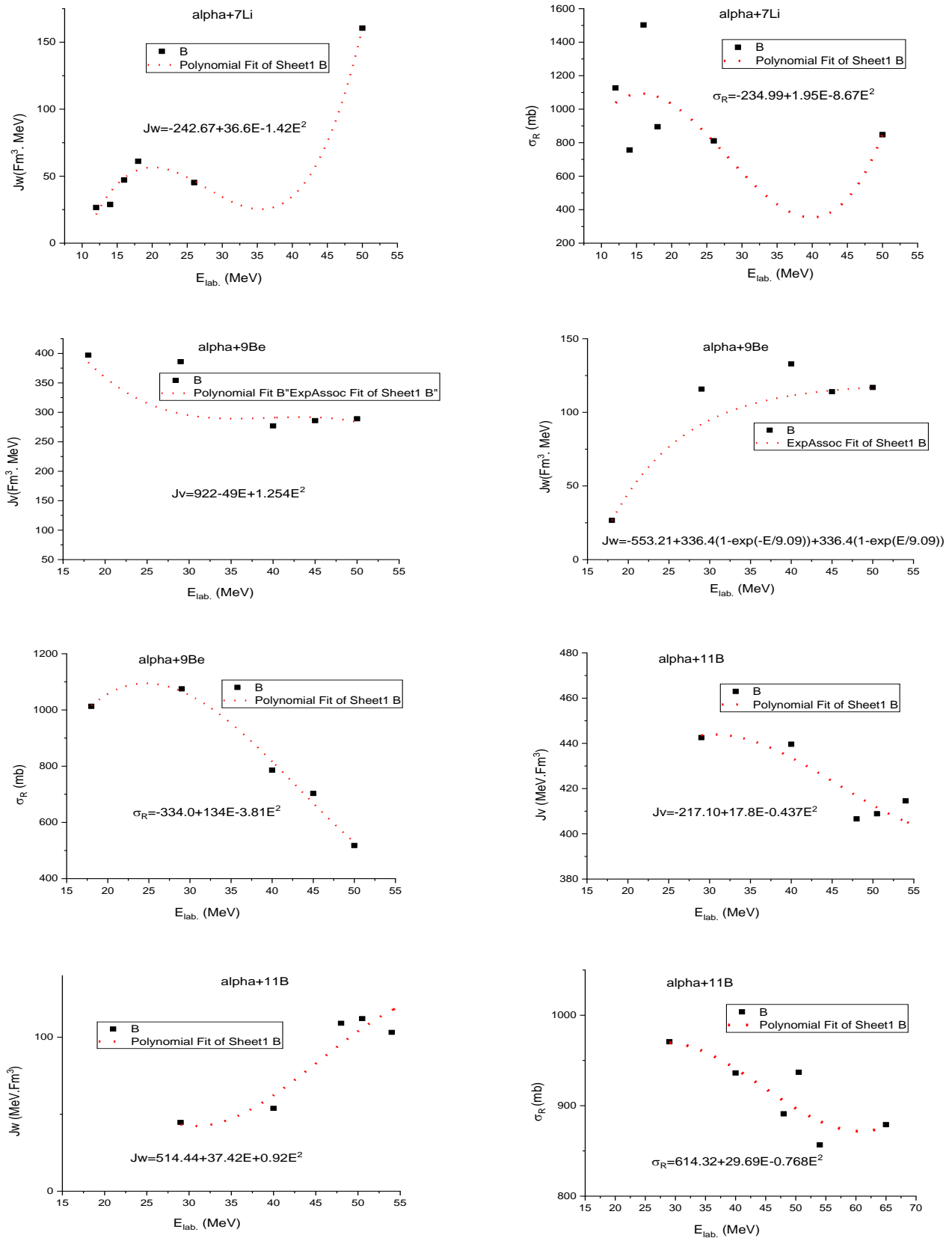


Fig. (7): Energy dependence of the total cross-section and volume integrals for the real and imaginary parts of the CM potentials per nucleon pair for α -particles elastically scattered by ${}^6\text{Li}$ and ${}^9\text{Be}$, ${}^7\text{Li}$ and ${}^{11}\text{B}$ nuclei

4. CONCLUSIONS

An analysis for alpha elastically scattered by ${}^6\text{Li}$, ${}^9\text{Be}$, and ${}^{11}\text{B}$ has been achieved using novel models: CM and CRC. The study has been achieved using CM as the real part and WS form as the imaginary part. The depth and diffuseness of the imaginary part were examined to reproduce differential cross-sections for alpha elastically scattered by ${}^6\text{Li}$, ${}^9\text{Be}$, and ${}^{11}\text{B}$. The depth has been increased, whereas the diffuseness was decreased to the minimum value for alpha elastically scattered by ${}^{11}\text{B}$ to 0.20, indicating the roughness of the nucleus. Twenty-five sets of scattering data for alpha elastically scattered by ${}^6\text{Li}$, ${}^9\text{Be}$, and ${}^{11}\text{B}$ have been investigated, where the normalization factor has a discrepancy for ${}^6\text{Li}$. The normalization factor is small at lower energies for ${}^7\text{Li}$, ${}^9\text{Be}$, and ${}^{11}\text{B}$. It increases with increasing energy, indicating the role of the model in such an important factor. The obtained values of the normalization factor using CM differ from the coupled reaction method, demonstrating the deepness of the potential with energy increasing. The light nuclei tendency to form clusters is obvious in this analysis. For the considered four nuclear systems, it was noticed that the volume integrals of real potential J_v smoothly decrease with increasing alpha energy, while the volume integrals of imaginary potential J_w , sharply increase with increasing alpha energy. The CM applicability on alpha elastically scattered by ${}^9\text{Be}$ and ${}^{11}\text{B}$ is restricted by the energy of alpha particles.

REFERENCES

- [1] Guardiola, R., I. Moliner, and M. Nagarajan, *Alpha-cluster model for 8Be and 12C with correlated alpha particles*. Nuclear Physics A, 2001. **679**(3-4): p. 393-409.
- [2] Amar, A., *Spectroscopic information of 6Li from elastic scattering of deuterons, ${}^3\text{He}$ and ${}^4\text{He}$ by ${}^6\text{Li}$* . International Journal of Modern Physics E, 2014. **23**(08): p. 1450041.
- [3] Amar, A. and O. Hemeda, *Crystalline Model Approach for Studying the Nuclear Properties of Light Nuclei*. International Journal of Nuclear and Quantum Engineering, 2021. **15**(2): p. 50-53.
- [4] Lähde, T.A., et al., *Lattice effective field theory for medium-mass nuclei*. Physics Letters B, 2014. **732**: p. 110-115.
- [5] Jensen, Ø., et al., *Computation of spectroscopic factors with the coupled-cluster method*. Physical Review C, 2010. **82**(1): p. 014310.
- [6] Hagen, G. and N. Michel, *Elastic proton scattering of medium mass nuclei from coupled-cluster theory*. Physical Review C, 2012. **86**(2): p. 021602.
- [7] Navratil, P., R. Roth, and S. Quaglioni, *Ab initio many-body calculation of the ${}^7\text{Be}$ (p, γ) ${}^8\text{B}$ radiative capture*. Physics Letters B, 2011. **704**(5): p. 379-383.
- [8] Navratil, P. and S. Quaglioni, *Ab Initio Many-Body Calculations of the ${}^3\text{H}$ (d, n) ${}^4\text{He}$ and ${}^3\text{He}$ (d, p) ${}^4\text{He}$ Fusion Reactions*. Physical Review Letters, 2012. **108**(4): p. 042503.
- [9] Lage, M., U. G. Meißner, and A. Rusetsky, *A method to measure the antikaon-nucleon scattering length in lattice QCD*. Physics Letters B, 2009. **681**(5): p. 439-443.
- [10] Bernard, V., et al., *Scalar mesons in a finite volume*. Journal of High Energy Physics. **2011**(1): p. 19.
- [11] Meyer, H.B., *Photodisintegration of a Bound State on the Torus*. arXiv preprint arXiv:1202.6675, 2012.
- [12] Briceno, R.A. and Z. Davoudi, *Moving multichannel systems in a finite volume with application to proton-proton fusion*. Physical Review D, 2013. **88**(9): p. 094507.
- [13] Rupak, G. and D. Lee, *Radiative capture reactions in lattice effective field theory*. Physical Review Letters, 2013. **111**(3): p. 032502.
- [14] Meißner, U.-G., *Clustering in nuclei from ab initio nuclear lattice simulations*. arXiv preprint arXiv:1509.08290, 2015.
- [15] Eldyshev, Y.N., V. Luk'yanov, and Y.S. Pol, *Analysis of elastic electron scattering on light nuclei on the basis of symmetrized fermi-density distribution*. 1972, Joint Institute. for Nuclear Research, Dubna, USSR.
- [16] Thompson, I., *Fresco 2.0*. 2006, Department of Physics, University of Surrey, Guildford GU2 7XH, England.

- [17] Bespalova, O., E. Romanovsky, and T. Spasskaya, *Nucleon–nucleus real potential of Woods–Saxon shape between– 60 and + 60 MeV for the $40 \leq A \leq 208$ nuclei*. Journal of Physics G: Nuclear and Particle Physics, 2003. **29**(6): p. 1193.
- [18] Matsuki, S., et al., *Elastic and Inelastic Scattering of 14.7 MeV Deuterons and of 29.4 MeV Alpha-Particles by $Li6$ and $Li7$* . Journal of the Physical Society of Japan, 1969. **26**(6): p. 1344-1353.
- [19] Bingham, H., K. Kemper, and N. Fletcher, *Elastic scattering of $4He$ from $6Li$ and $7Li$ at 12.0 to 18.5 MeV*. Nuclear Physics A, 1971. **175**(2): p. 374-384.
- [20] Green, P., et al., *Analyzing powers in 4He ($6Li \rightarrow, Li 6$) $4He$* . Physical Review C, 1996. **53**(6): p. 2862.
- [21] Watters, H.J., *Elastic and Inelastic Scattering of 31.5-Mev Alpha Particles by Light Nuclei*. Physical Review, 1956. **103**(6): p. 1763.
- [22] Hauser, G., et al., *Elastic scattering of 104 MeV alpha particles*. Nuclear Physics A, 1969. **128**(1): p. 81-109.
- [23] Burkova, N., M. Zhusupov, and R. Kabatayeva, *A potential description of α -particle elastic scattering by the 6Li and 7Li nuclei*. Bulletin of the Russian Academy of Sciences: Physics, 2012. **76**(10): p. 1066-1069.
- [24] Heusi, P., et al., *sup $6/Li$ - cap alpha. scattering below 3 MeV*. Nuclear Physics A; 1981. **357**(2).
- [25] Blieden, H., G. Temmer, and K. Warsh, *A study of the 9Be (p, α) 6Li reaction from 3.5 to 12.5 MeV*. Nuclear Physics, 1963. **49**: p. 209-238.
- [26] Bragin, V., et al., *Exchange effect role in elastic scattering of α -particles and 3He ions on $6Li$ nuclei*. Yadernaya Fizika, 1986. **44**(2): p. 312-319.
- [27] Foroughi, F., E. Bovet, and C. Nussbaum, *Elastic and inelastic scattering of alpha particles from $6Li$ at 59MeV*. Journal of Physics G: Nuclear Physics, 1979. **5**(12): p. 1731.
- [28] Burtebaev, N., et al., *Elastic and inelastic scattering of 50-MeV alpha particles by $6Li$ and $7Li$ nuclei: The role of exchange effects in anomalous scattering at large angles*. Physics of Atomic Nuclei, 1996. **59**.
- [29] Samanta, C., et al., *Alpha-particle scattering from $Li 6$ near the α -d breakup threshold*. Physical Review C, 1992. **45**(4): p. 1757.
- [30] Han, Y., Y. Shi, and Q. Shen, *Deuteron global optical model potential for energies up to 200 MeV*. Physical Review C, 2006. **74**(4): p. 044615.
- [31] Rusek, K., et al., *Scattering of polarized 7Li from 4He* . Physical Review C, 2003. **67**(1): p. 014608.
- [32] Matsuki, S., *Disintegration of 7Li and 6Li by 29.4 MeV Alpha-Particles*. Journal of the Physical Society of Japan, 1968. **24**(6): p. 1203-1223.
- [33] Taylor, R., N. Fletcher, and R. Davis, *Elastic scattering of 4–20 MeV alpha particles by 9Be* . Nuclear Physics, 1965. **65**(2): p. 318-328.
- [34] Roy, S., et al., *Coupled channel folding model description of α scattering from 9Be* . Physical Review C, 1995. **52**(3): p. 1524.
- [35] Lukyanov, S., et al., *Study of internal structures of 9, 10Be and 10B in scattering of $4He$ from $9Be$* . Journal of Physics G: Nuclear and Particle Physics, 2014. **41**(3): p. 035102.
- [36] Lucas, B., S. Cosper, and O. Johnson, *Scattering of 18.4-MeV Alpha Particles by Beryllium*. Physical Review, 1964. **133**(4B): p. B963.
- [37] Burtebayev, N., et al. *Elastic scattering of alpha particles from $9Be$ in the framework of optical model*. in *Journal of Physics: Conference Series*. 2020. IOP Publishing.
- [38] Peterson, R., *Alpha-particle scattering from $9Be$* . Nuclear Physics A, 1982. **377**(1): p. 41-52.
- [39] Burtebayev, N., et al. *Investigation of the elastic and inelastic scattering of $4He$ from $11B$ in the energy range 29-50.5 MeV*. in *Journal of Physics: Conference Series*. 2018. IOP Publishing.
- [40] Burtebaev, N., et al., *Scattering of α particles on $11B$ nuclei at energies 40 and 50 MeV*. Physics of Atomic Nuclei, 2005. **68**(8): p. 1303-1313.
- [41] Abele, H., et al., *Measurement and folding-potential analysis of the elastic α -scattering on light nuclei*. Zeitschrift für Physik A Atomic Nuclei, 1987. **326**(4): p. 373-381.
- [42] Danilov, A., et al., *Study of rlastic and inelastic $11B + \alpha$ scattering and search for cluster states of enlarged radius in $11B$* . Physics of Atomic Nuclei, 2015. **78**(6): p. 777-793.